AIP | Journal of Applied Physics

Observation of spin glass state in weakly ferromagnetic Sr2FeCoO6 double perovskite

R. Pradheesh, Harikrishnan S. Nair, C. M. N. Kumar, Jagat Lamsal, R. Nirmala et al.

Citation: J. Appl. Phys. **111**, 053905 (2012); doi: 10.1063/1.3686137
View online: http://dx.doi.org/10.1063/1.3686137
View Table of Contents: http://jap.aip.org/resource/1/JAPIAU/v111/i5
Published by the American Institute of Physics.

Observation of spin glass state in weakly ferromagnetic Sr_2FeCoO_6 double perovskite

R. Pradheesh,[1] Harikrishnan S. Nair,[2] C. M. N. Kumar,[2] Jagat Lamsal,[3] R. Nirmala,[1] P. N. Santhosh,[1] W. B. Yelon,[4] S. K. Malik,[5] V. Sankaranarayanan,[1,a)] and K. Sethupathi[1,a)]
[1]*Low Temperature Physics Laboratory, Department of Physics, Indian Institute of Technology Madras, Chennai 600036, India*
[2]*Jülich Center for Neutron Sciences-2/Peter Grünberg Institute-4, Forschungszentrum Jülich, 52425 Jülich, Germany*
[3]*Department of Physics and Astronomy, University of Missouri-Columbia, Columbia, Missouri 65211, USA*
[4]*Materials Research Center and Department of Chemistry, Missouri University of Science and Technology, Rolla, Missouri 65409, USA*
[5]*Departmento de Fisica Teórica e Experimental, Natal-RN, 59072-970, Brazil*

(Received 30 September 2011; accepted 18 January 2012; published online 1 March 2012)

A spin glass state is observed in the double perovskite oxide Sr_2FeCoO_6 prepared through sol-gel technique. Initial structural studies using x rays reveal that the compound crystallizes in tetragonal $I4/m$ structure with lattice parameters, $a = 5.4609(2)$ Å and $c = 7.7113(7)$ Å. The temperature dependent powder x ray diffraction data reveal no structural phase transition in the temperature range 10-300 K. However, the unit cell volume shows an anomaly coinciding with the magnetic transition temperature thereby suggesting a close connection between lattice and magnetism. Neutron diffraction studies and subsequent bond valence sums analysis show that in Sr_2FeCoO_6, the B site is randomly occupied by Fe and Co in the mixed valence states of Fe^{3+}/Fe^{4+} and Co^{3+}/Co^{4+}. The random occupancy and mixed valence sets the stage for inhomogeneous magnetic exchange interactions and in turn, for the spin glass state in this double perovskite, which is observed as an irreversibility in temperature dependent dc magnetization at $T_f \sim 75$ K. Dynamical scaling analysis of $\chi'(T)$ yields a critical temperature $T_{ct} = 75.14(8)$ K and an exponent $z\nu = 6.2(2)$ typical for spin glasses. The signature of presence of mixed magnetic interactions is obtained from the thermal hysteresis in magnetization of Sr_2FeCoO_6. Combining the neutron and magnetization results of Sr_2FeCoO_6, we deduce that Fe is in low spin state while Co is in both low spin and intermediate spin states. © *2012 American Institute of Physics*. [doi:10.1063/1.3686137]

I. INTRODUCTION

Ferromagnetic double perovskite oxides of general formula $A_2BB'O_6$ (where A = divalent alkaline earth; B and B' = transition metal ions) have been extensively studied as candidates for magnetoresistive materials.[1,2] The crystallographic ordering of the B cations in these compounds plays an important role in realizing novel magnetic and transport properties including magnetoresistance.[2] Depending on the crystallographic arrangement of B cations, double perovskites are classified as random, rock salt or layered.[3] For example, Ca_2FeReO_6 has rock salt arrangement[4] while $PrBaCo_2O_{5+\delta}$ adopts layered structure.[5] Though B site ordered double perovskites are of interest for magnetoresistive and ferromagnetic (FM) properties, it has been observed that comparable ionic radii and oxidation states of different cations at the B site can lead to mixed crystallographic occupation and result in what is known as antisite disorder.[3] Depending on the type, size and charge of the cations present at the B site, different magnetic properties varying from antiferromagnetism[6,7] (AFM) to spin glass[8,9] (SG) have been reported in double perovskites. Most of the Fe based double perovskites display a high magnetic transition temperature, which is surprising given the fact that the Fe ions are separated far apart in these materials.[2] However, a few exceptions (like Sr_2FeWO_6) to this have been reported with low magnetic transition temperatures ≈ 37 K.[10] The correlation between magnetoresistance and magnetism in these compounds and the site disorder is understood from the studies on ordered and disordered Sr_2FeMoO_6.[11] The site disorder can partially or completely destroy the B site ordering of cations and can influence the physical properties like magnitude of magnetization, Curie temperature and low-field magnetoresistance.[12,13] It has been found that the site disorder can be influenced by preparative conditions such as heat treatment temperature,[12,14] treatment time[14] etc. Therefore, it is possible to tune the magnetic properties of $A_2BB'O_6$ through suitable selection of B/B' cations and preparative conditions. Though double perovskite oxides in the $A_2BB'O_6$ family have been actively investigated, there are only a few reports on the Co based double perovskite, Sr_2FeCoO_6.[15,16] Earlier studies on the chemically similar single perovskite $SrFe_{1-x}Co_xO_3$ [$x = 0.5$] reported a high T_c of 340 K and saturation magnetization of 3 μ_B.[17,18] Meanwhile, Maignan *et al.*, reported $SrFe_{0.5}Co_{0.5}O_3$ to be ferromagnetic below $T_c \sim 200$ K with a saturation magnetization of 1.5 μ_B at 5 K.[15] *Ab initio* band structure calculations on Sr_2FeCoO_6 showed that both Co and Fe make comparable contributions to ferromagnetism of the compound[19] where $Co^{4+}(d^5\bar{L})$ and $Fe^{4+}(d^4\bar{L})$ in high spin (HS) states can lead to metallicity and ferromagnetism.

a)Electronic addresses: vsn@physics.iitm.ac.in and ksethu@physics.iitm.ac.in.

However, owing to the comparable ionic radii and valence states of Fe and Co (both in 4 + state), it is surprising that Co doped $SrFeO_3$ showed ferromagnetism. The absence of a linear *B*-O-*B*′-O-*B* chain consequent to tilts in the BO_6 and $B'O_6$ octahedra can cause 90° and 180° superexchange interactions.[20,21] Moreover, comparable ionic radii of the *B* site cations combined with antisite disorder can lead to magnetic frustration in the double perovskites. Cluster glass phenomenon in $Sr_2Mn_{1-x}Fe_xMoO_6$ (Ref. 20) was attributed to the local magnetic frustration developed due to the competing nearest neighbor (*NN*) and next nearest neighbor (*NNN*) superexchange interactions. Incompatible superexchange interactions and magnetic frustration due to the site disorder of the *B* and *B*′ cations were observed in $Sr_2FeTiO_{6-\delta}$.[22] These observations point to the fact that mixed valence state of the *B* and *B*′ ions and their crystallographic disorder can lead to a spin glass state as it would create *mixed interactions* and *randomness*.[23] In the present study on Sr_2FeCoO_6, through detailed structural and magnetic investigations, we observe an inhomogeneous magnetic state with the characteristics of a spin glass phase arising from incompatible magnetic interactions and crystallographic disorder.

II. EXPERIMENTAL DETAILS

Polycrystalline samples of Sr_2FeCoO_6 were prepared by sol-gel method as described elsewhere.[24] The gel was dried at 120 °C and the final sintering of the sample was done at 1050 °C for 36 h. Powder x ray diffraction patterns were recorded in the temperature range of 10-300 K using a Huber diffractometer (Mo K_α) in Guinier geometry. Neutron powder diffraction (NPD) measurement at 300 K was performed with neutron wavelength of 1.4789 Å at the University of Missouri Research Reactor (MURR) employing position sensitive detector. The crystal structure was refined by Rietveld method[25] using FULL-PROF program.[26] dc and ac magnetic measurements were carried out in a commercial superconducting quantum interference device (SQUID) magnetometer and physical property measurement system (both M/s Quantum Design, USA). dc magnetization in field cooled (FC) and zero-field cooled (ZFC) cycles were performed at different applied fields from 100 Oe to 50 kOe. ac susceptibility was measured using SQUID magnetometer in an ac field of 3 Oe with frequencies of 33, 133, 337, 667, 967, and 1333 Hz.

III. RESULTS AND DISCUSSION

Using the powder XRD data, the crystal structure of Sr_2FeCoO_6 was refined in the tetragonal space group *I*4/*m* (No. 87) with lattice constants $a = 5.4568(2)$ Å and $c = 7.7082(4)$ Å. A pictorial representation of the Sr_2FeCoO_6 double perovskite unit cell is shown in Fig. 1. Even though, following the earlier reports on $SrFe_{1-x}Co_xO_3$ (Ref. 15) a refinement in cubic $Pm\bar{3}m$ space group was undertaken initially, an improved fit to XRD data was achieved using the tetragonal space group. The results of the Rietveld analysis are presented in Fig. 2(a) where the observed XRD pattern at 300 K, the calculated profile, difference profile, and the Bragg peaks are shown. The inset (1) of Fig. 2(a) compares the goodness-of-fit (χ^2) of the refinement for *I*4/*m* and $Pm\bar{3}m$ space groups, and it is found that the former gives a better fit. The temperature evolution of unit cell volume is presented in Fig. 2(b). The variation of cell volume was modeled using the Grüneisen approximation,[27]

$$V(T) = \gamma U(T)/K_0 + V_0;$$
$$U(T) = 9Nk_BT(T/\Theta_D)^3 \int_0^{\Theta_D/T} x^3/(e^x - 1)dx.$$

Here, U(T) is the specific internal energy, γ is the Grüneisen parameter, K_0 is the incompressibility, V_0 is the volume at $T = 0$ K, and Θ_D is the Debye temperature. The resulting fit is shown as a solid line in Fig. 2(b). Note that the fit deviates from the data at $T \sim 75$ K where the volume displays a hump-like feature (a magnified low-temperature region where the fit deviates from the data is shown in the inset (1)). This is inferred as magnetoelastic or magnetovolume effect coinciding with the magnetic transition. In this respect, further studies aimed at investigating magneto-structural coupling and polarization measurements would be rewarding. The value of Θ_D obtained from the fit is 463 K[21] and $V_0 = 227.89$ Å^3. The Θ_D of Sr_2FeCoO_6 lies in the range of values estimated for double perovskites like Sr_2FeTeO_6 assuming two different Θ_D's for light and heavy atoms.[28] In Fig. 2(c) we show the temperature variation of the lattice parameters *a* and *c*. An important structural parameter characterizing the double perovskites, and having a bearing on the magnetic properties is the cationic site disorder. However,

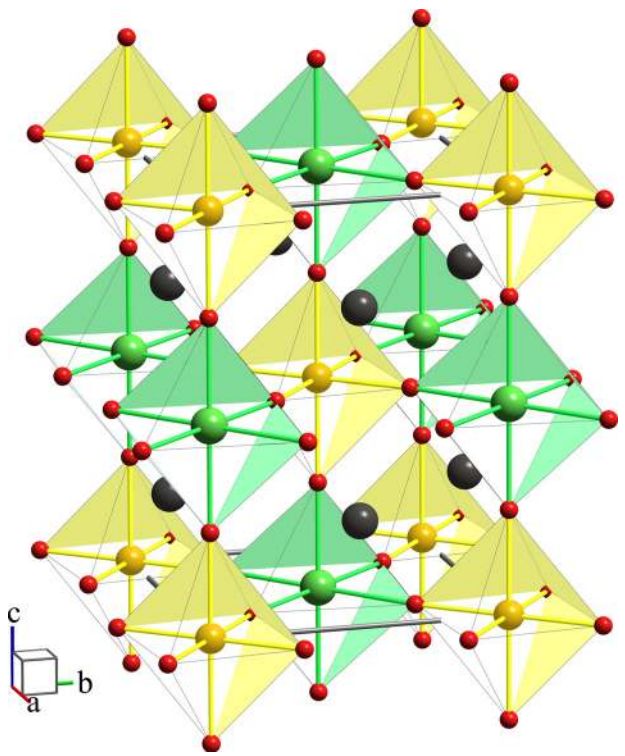

FIG. 1. (Color online) The tetragonal structure of the double perovskite Sr_2FeCoO_6. The CoO_6 and FeO_6 octahedra are shown with Fe (Co) at the center surrounded by the oxygen. For succinctness the structure shown is of the *B* site ordered type.

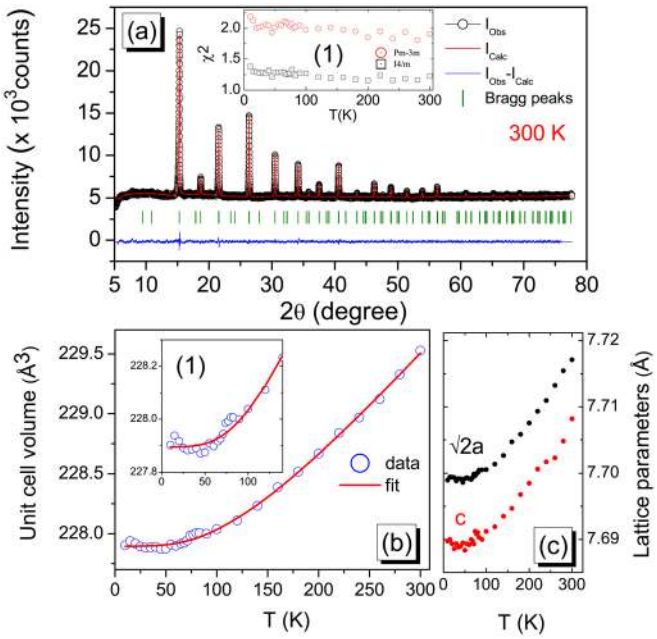

FIG. 2. (Color online) (a) X-ray diffraction pattern of Sr_2FeCoO_6 at 300 K refined in tetragonal *I*4/*m* space group. Inset (1) compares the goodness-of-fit of the refinement in two space groups. Quality measures of refinement are $R_{wP} = 1.52\%$, $R_P = 1.18\%$, $\chi^2 = 1.23$. (b) shows the analysis of unit cell volume using Grüneisen approximation. Inset (1) shows the enlarged view of the anomaly near 75 K. (c) shows temperature evolution of lattice parameters $\sqrt{2a}$ and c (the error bars were smaller than the size of the data markers).

since the x-ray atomic structure factors of Fe and Co are comparable, an accurate evaluation of atomic occupancies was not possible from the present XRD data.

In order to check the degree of *B* site ordering and to confirm the crystal structure of Sr_2FeCoO_6 determined from XRD data, we performed neutron diffraction experiments (the neutron coherent scattering cross section of Fe and Co are 11.22×10^{-24} cm^2 and 0.779×10^{-24} cm^2, respectively).[29] In Fig. 3 we present the neutron diffraction pattern of Sr_2FeCoO_6 collected at 300 K along with the results of structure refinement using *I*4/*m* space group. Our Mössbauer studies confirm that Fe occupies two distinct crystallographic sites and hence the choice of *I*4/*m* space group was made in our structural analysis. We carried out the refinement of

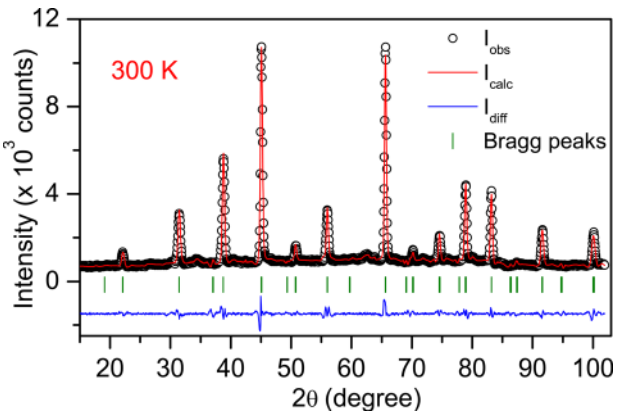

FIG. 3. (Color online) (a) Observed (I_{obs}), calculated (I_{calc}) and difference (I_{diff}) profiles of neutron diffraction pattern of Sr_2FeCoO_6 at 300 K refined in tetragonal *I*4/*m* space group. Vertical markers correspond to Bragg peaks. Quality measures of refinement are $R_{wP} = 17.6\%$, $R_P = 14.6\%$, $\chi^2 = 3.38$.

atomic occupancies using structural models assuming ordered as well as disordered cationic arrangement at the B/B' site. A better fit to the experimental data, in terms of profile-match and discrepancy factors, was achieved by assuming a disordered model with a random arrangement for the B/B' cations. The oxygen content was quantified in the refinement process and the deviation from stoichiometry (δ) was found to be 0.11. The structural parameters of Sr_2FeCoO_6 including atomic positions, lattice parameters and occupancies and the bond valence sums (BVS) calculated using VaList program[31] are collected in Table I. A rock-salt arrangement of the cations in double perovskites normally occurs if the charge difference between the *B* and *B'* is greater than 2.[3] In the case of Sr_2FeCoO_6, the charge difference is close to unity as clear from Table I. The BVS calculations give an insight into the oxidation state of the ions and reasonably support random occupancy at the B/B' site and mixed valence of Fe and Co. The bond length Fe(2)-O(2) estimated from the structural analysis is 1.969 Å and is comparable to the values found in the literature for double perovskites, especially $Sr_2Fe_{0.75}Cr_{0.25}MoO_6$ (Fe-O distance is 1.968 Å).[32] The bond lengths and bond angles of Sr_2FeCoO_6 obtained from the analysis of NPD data are given in Table II. According to Glazer's notation, the space group *I*4/*m* has an antiphase tilting along *c* axis denoted as $a^0a^0c^-$, which represents the small shifts of the in-plane oxygen atoms.[33] The magnitude of tilting can be derived from Fe-O-Co (ϕ) angle as $(180 - \phi)/2 = 1.04°$. The average bond length of ⟨Fe1-O⟩ and ⟨Fe2-O⟩ are 1.9147 Å and 1.9573 Å, where the latter bond length compare well with the expected value calculated as the sum of the ionic radii of Fe^{3+} in low spin state (LS) ($r_{LS}^{Fe} = 0.55$ Å) and O^{2-} ($r_O = 1.40$ Å).[34] Similarly the bond length values for ⟨Co1-O⟩ (1.9147 Å) and ⟨Co2-O⟩ (1.9573 Å) are close to the values of the calculated bond length if we assume cobalt has a low spin 4 + valence state ($r_{LS}^{Co} = 0.518$ Å) (Ref. 35) and an intermediate spin (IS) 3 + state ($r_{IS}^{Co} = 0.56$ Å) respectively.[36]

The magnetization of Sr_2FeCoO_6 measured at 500 Oe in the zero field-cooled (ZFC) as well as field-cooled cooling (FC) and warming (FCW) cycles are shown in Fig. 4(a). A magnetic transition is evident at $T_c \sim 75$ K. The low temperature magnetization data show a marked irreversibility below T_c indicating the presence of a weak component of ferromagnetism as suggested by Goodenough-Kanamori rules for the $d^4 - d^5$ cation-anion-cation superexchange[37,38] or spin glass state. With an increase in applied field, the ZFC/FC curves tend to merge and the FC arm shows signs of saturation with broadening of the peak (see inset (1), Fig. 4(a)). This broadening is also evident in inset (2), Fig. 4(a) where the FC magnetization at higher fields is presented. It signifies the presence of majority FM phase since for an antiferromagnet the increase in the field would have had little effect on the sharpness of the transition.[39] The inverse magnetic susceptibility in the temperature range 220- 350 K was fitted to Curie-Weiss law and the result is presented in Fig. 4(b). A deviation from the Curie-Weiss (CW) law can be clearly seen for temperatures significantly above T_c also. Such deviations from Curie- Weiss behavior above T_c attributed to antiferromagnetic spin fluctuations are commonly observed in spin glass systems.[40] Previous reports show that Fe and

TABLE I. Occupancy and bond valence sums (BVS) and (x, y, z) values obtained after Rietveld refinement of the neutron data at 300 K. The unit cell parameters are $a = 5.4609(2)$ Å, $b = 5.4609(2)$ Å, and $c = 7.7113(7)$ A. The quality of the fit is indicated by the discrepancy factors, $R_{WP} = 17.6\%$, $R_P = 14.6\%$, and the goodness-of-fit, $\chi^2 = 3.38$.

Atom	Site	X	y	z	Occupancy	BVS
Sr	4*d*	0	0.5	0.25	0.25	2.336(9)
Fe1/Co1	2*a*	0	0	0	0.0625	4.055(69)/3.650(62)
Fe2/Co2	2*b*	0	0	0.5	0.0625	3.51(41)/2.967(54)
O1	4*e*	0	0	0.24739(3)	0.25994(10)	1.970(38)
O2	8*h*	0.26798(13)	0.21981(18)	0	0.47621(6)	1.985(15)

Co in $SrFe_{1-x}Co_xO_3$ solid solutions can possess complex valence states[41] and that, Fe-O-Co superexchange path-ways can favor electronic transfer from Fe^{3+} high spin state (HS, S = 5/2) to Co^{4+} low spin state (LS, S = 1/2).[15] Complex valence states are observed in the case of Sr_2FeCoO_6 from the CW analysis of magnetic susceptibility and is described in detail below.

The effective paramagnetic moment calculated from the CW analysis is $\mu_{eff} = 3.9\ \mu_B$. Keeping in mind that the system is randomly ordered, the effective magnetic moment can be calculated by assuming 50% of Fe and Co (in both 2*a* and 2*b* sites) in 4 + and 3 + spin states. The experimentally obtained effective spin-only moment from the CW fit lies in between the theoretical spin-only moment values of $\mu_{eff} = 3.67\ \mu_B$ and $\mu_{eff} = 4.12\ \mu_B$ (see, Table III). Comparing this with the bond length values obtained we infer that Co^{3+} is in intermediate spin state while Fe^{3+}, Fe^{4+} and Co^{4+} are in low spin state. The positive value of Curie-Weiss temperature, $\Theta_{CW} = 99$ K, calculated from the fit confirms the presence of ferromagnetic interactions in the system. This value is lower than that reported earlier for $SrFe_{0.5}Co_{0.5}O_{3-\delta}$ where the role of oxygen non-stoichiometry on ordering temperature was discussed.[41] However, oxygen deficient double perovskites exhibit very low magnetoresistance (MR), which is not the case in Sr_2FeCoO_6 since we have observed 63% MR at 12 K at an applied field of 12 T.[30]

Figure 4(c) shows the plot of FCC and FCW magnetization curves measured at 100 Oe where a clear thermal hysteresis below T_c is discernible. Thermal hysteresis in magnetization cycles are related to the presence of first-order phase transitions with mixed magnetic phases as has been reported in the case of disordered manganites[42,43] or rare earth double perovskites.[44]

The end compositions of Sr_2FeCoO_6, viz., $SrFeO_3$ and $SrCoO_3$ possess helical and collinear ferromagnetic magnetic structures, respectively. Hence, Sr_2FeCoO_6 could consist of AFM regions where Fe-O-Fe superexchange dominate and Fe-O-Co FM regions, which is an ideal scenario for the formation of spin glass phase. Magnetic frustration effects in double perovskite oxides are also reported to show similar thermal hysteresis below T_c as in the case of Sr_2MReO_6 (M = Sc, Co etc).[45] Drawing parallels, magnetic frustration effects in Sr_2FeCoO_6 originating from different exchange paths due to multiple valences of Co/Fe can also lead to such effects. We also note that at higher applied fields like 500 Oe (Fig. 4(a)), the hysteresis is absent. These features indicate a weak first-order-like phase transition due to the presence of mixed magnetic phases.

The isothermal magnetization curve of Sr_2FeCoO_6 at 2 K is shown in the main panel of Fig. 5(a). The inset (1) presents the $M(H)$ curves at 5 K, 10 K and the inset (2) those in the range 30-300 K. Hysteresis is observed below 50 K indicating weak ferromagnetism at low temperature. A decrease in remanance and coercivity is observed with an increase in temperature (Fig. 5(b)). As the temperature increases, the irreversibility reduces and becomes sigmoidal at 50 K and above; whereas no saturation of magnetization is attained even at an applied field of 50 kOe. A notable feature in the isothermal magnetization curves is the step like

TABLE II. Selected bond angles and bond lengths of Sr_2FeCoO_6 obtained from the structural analysis.

Fe1/Co1-O1	1.9227(15) × 2
Fe1/Co1-O2	1.9107(15) × 4
Fe2/Co2-O1	1.9329(15) × 2
Fe2/Co2-O2	1.9695(15) × 4
Fe1-O2-Co2	177.92(1)

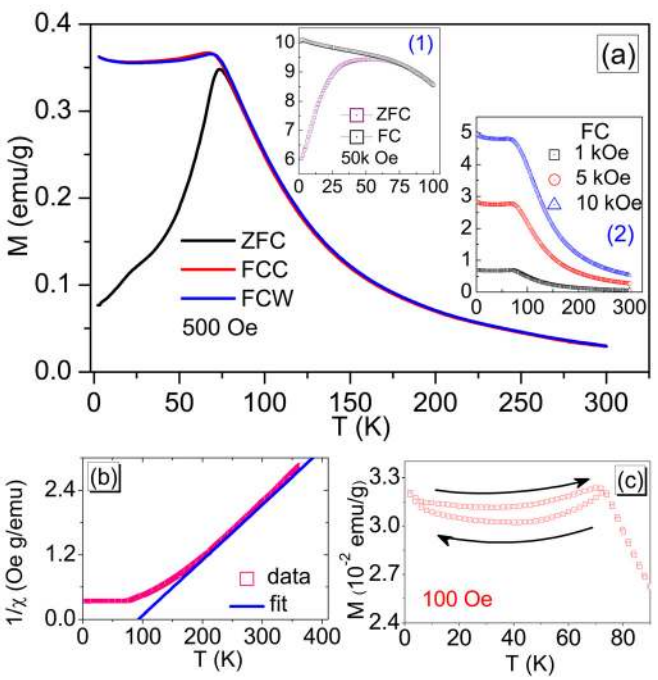

FIG. 4. (Color online) (a) Zero field cooling (ZFC), field cooled cooling (FC), and warming (FCW) cycles of magnetization of Sr_2FeCoO_6 as a function of temperature at 500 Oe. Inset (1) shows the ZFC/FC curves at 50 kOe and (2) FC curves at different applied fields. (b) Temperature dependence of inverse magnetic susceptibility along with Curie-Weiss fit. (c) Thermal hysteresis observed in FC data at 100 Oe.

TABLE III. Calculated spin only moments ($\mu_{SO}^2 = \mu_{2a}^2 + \mu_{2b}^2$) for Sr_2FeCoO_6 assuming the possible spin state values. The calculated spin only moment (μ_{so}) lies in between the last two configurations. Note that Co^{3+} HS $S=2$, LS $S=0$, IS $S=1$; Co^{4+} HS $S=5/2$, IS $S=3/2$, LS $S=1/2$; Fe^{3+} HS $S=5/2$, LS $S=1/2$; Fe^{4+} HS $S=2$, LS $S=1$.

2a	2b	$\mu_{SO}(\mu_B)$
$Co^{4+}{}_{HS}(S=5/2)$; $Fe^{4+}{}_{HS}(S=2)$	$Co^{4+}{}_{HS}(S=5/2)$; $Fe^{4+}{}_{HS}(S=2)$	7.68
$Co^{3+}{}_{HS}(S=2)$; $Fe^{4+}{}_{HS}(S=2)$	$Co^{4+}{}_{HS}(S=5/2)$; $Fe^{4+}{}_{HS}(S=5/2)$	7.68
$Co^{4+}{}_{HS}(S=5/2)$; $Fe^{4+}{}_{LS}(S=1)$	$Co^{4+}{}_{HS}(S=5/2)$; $Fe^{4+}{}_{LS}(S=1)$	6.56
$Co^{4+}{}_{LS}(S=1/2)$; $Fe^{4+}{}_{HS}(S=2)$	$Co^{4+}{}_{LS}(S=1/2)$; $Fe^{4+}{}_{HS}(S=2)$	5.19
$Co^{4+}{}_{LS}(S=1/2)$; $Fe^{4+}{}_{LS}(S=1)$	$Co^{4+}{}_{LS}(S=1/2)$; $Fe^{4+}{}_{LS}(S=1)$	3.32
$Co^{4+}{}_{LS}(S=1/2)$; $Fe^{4+}{}_{LS}(S=1)$	$Co^{3+}{}_{IS}(S=1)$; $Fe^{4+}{}_{LS}(S=1)$	3.67
$Co^{3+}{}_{IS}(S=1)$; $Fe^{4+}{}_{LS}(S=1)$	$Co^{4+}{}_{IS}(S=3/2)$; $Fe^{3+}{}_{LS}(S=1/2)$	4.12

behavior in magnetization at low fields as presented in the enlarged view in Fig. 5(c). Such a behavior was observed in Sr_2YRuO_6 and has been attributed to spin flop transition taking place at a critical field.[39] However, the aptness of such an explanation in the case of Sr_2FeCoO_6 cannot be tested until the magnetic structure is ascertained.

Sharpness of the peak in ac susceptibility curves and its shift to higher temperature with increasing frequency are typical features exhibited by SG systems.[23,46] In order to probe this, ac susceptibility measurements were performed in the temperature range 5–250 K, with a driving field of 3 Oe. Figure 6(a) shows the temperature dependence of the real part of ac susceptibility, $\chi'(T)$, at different applied frequencies in the range 33–1333 Hz (ω). $\chi'(T)$ attains a maximum at T_f, the freezing temperature that shifts to higher temperature as the frequency is increased. The shift of the peaks as a function of frequency is clear in Fig. 6(b) and is characteristic of spin glasses.[23] A fit of the ac susceptibility data to the Arrhenius relation, $f = f_0 \exp[E_a/k_BT]$, where E_a is the activation energy, yielded unphysical values of $f_0 = 10^{82}$ Hz and $E_a = 14\,301$ eV. The failure of Arrhenius relation points to SG behavior, since a description of mere energy-barrier blocking and thermal activation will not suit the SG transition. In order to confirm the spin glass behavior, analysis of the susceptibility data using the dynamical scaling relation at T_c was performed. For a spin glass, the maximum of $\chi'(T)$ (freezing temperature, T_f) depends on the applied frequency and the characteristic time, $t = 1/\omega$, is equal to the maximum relaxation time τ. Thus, a spin glass phase can be judged if τ follow a power law divergence of the form

$$\tau = \tau_0 \left(\frac{T_f}{T_{ct} - T_f} \right)^{zv},$$

where T_{ct} is the critical temperature and zv and τ_0 are the critical exponents and microscopic time scale, respectively.[23] The best fit to the above equation, as shown in Fig. 6(c) (inset presents the same graph in log-log scales), yields $zv = 6.2(2)$, $T_{ct} = 75.14(8)$ K, and $\tau_0 \approx 10^{-12}$ s. The values of τ_0 and zv are consistent with that of conventional 3 D spin glasses[47] and Fe doped cobaltites.[48] In order to probe whether the FM state coexist with the frozen spin glass state as in *reentrant* spin glasses, we performed ac susceptibility measurements with superimposed dc fields. The result is presented in Fig. 6(d), which shows the out of phase susceptibility in an external dc field varying from 50–1000 Oe at a frequency of 33 Hz with an ac amplitude of 3 Oe. We do not observe emergence of a second peak as observed in certain *reentrant* systems,[49] instead, the intensity of the peak at T_c in $\chi''(T)$ diminishes with increasing field indicating FM nature of the compound. Thus ac susceptibility studies confirm the presence of canonical SG state in Sr_2FeCoO_6, which in turn suggests the presence of disorder.

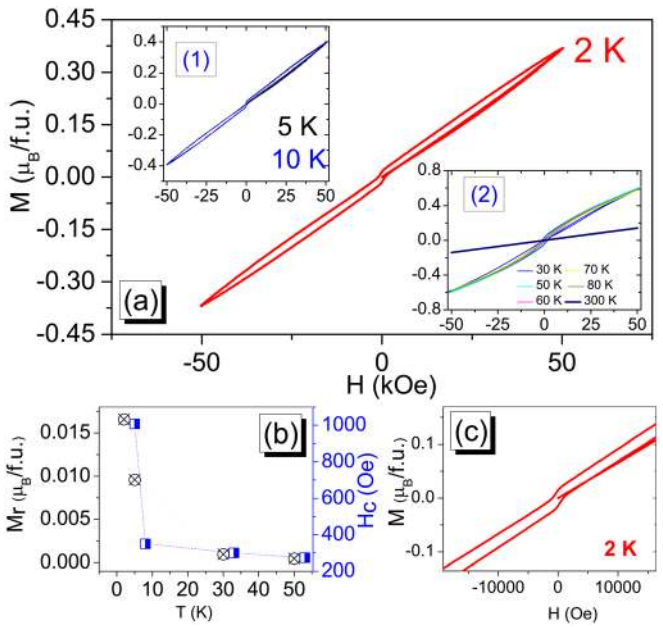

FIG. 5. (Color online) (a) Isothermal magnetization of Sr_2FeCoO_6 at 2 K. Insets (1) and (2) present isotherms at elevated temperatures. (b) Variation of remnant magnetization, M_r (circles) and coercive field, H_c (squares) with temperature. (c) An enlarged view of the magnetization isotherms at 2 K for low fields.

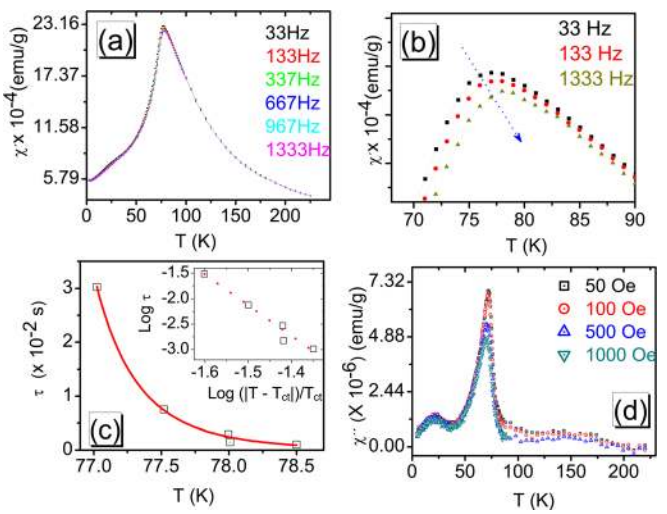

FIG. 6. (Color online) (a) Temperature dependence of ac susceptibility of Sr_2FeCoO_6 at different frequencies. (b) The peak in $\chi'(T)$ ~75 K, which shifts to higher temperature as the frequency is increased, signifying glassy magnetism. (c) The fit using the power law for critical slowing down, where the best fit gave $zv = 6.2$, $\tau_0 = 10^{-12}$ s. The inset presents the same plot but in log-log scale. (d) displays $\chi''(T)$ at different values of superimposed dc magnetic fields.

To summarize the results, Sr_2FeCoO_6 crystallizes in tetragonal *I*4/*m* structure where the *B* site is randomly occupied by Fe and Co in 2*a* and 2*b* sites. The assignment of *I*4/*m* space group is also supported by the bond valence sums analyses. The Fe and Co cations in Sr_2FeCoO_6 exist in mixed valence states of $+3$ and $+4$. The random crystallographic occupation and mixed valency sets the stage for mixed FM and AFM interactions between the transition metal cations and in turn, lead to inhomogeneous magnetic behavior in Sr_2FeCoO_6. In a perfectly ordered double perovskite, the magnetic exchange is predominantly governed by the ferromagnetic Fe^{3+}-$O^{2-}$$Co^{4+}$. With the occurrence of site disorder, additional antiferromagnetic exchange paths like Fe-Fe or Co-Co are introduced. The spin glass phase with a $T_f \sim 75$ K that appears in Sr_2FeCoO_6 has its origin in the multiple exchange paths that arise due to the mixed interactions. The magnetic moment of $0.39\mu_B$ at 5 K suggests that the transition metal ions in this compound are in a mixed valence state unlike high-spin tetravalent state in $SrFe_{0.5}Co_{0.5}O_3$.[50] The magnetic ordering of double perovskites is a function of the strength of the *NN* and *NNN* interactions[51] and the competition between these interactions is known to lead to magnetic frustration effects in Ln_2LiRuO_6 (Ln = Pr, Nd, Eu, Gd, Tb) (Ref. 52) and $LaBaCoNbO_6$.[53] Depending on the strength of *NN* and *NNN* interactions materials are classified as Type *I* (strength of *NNN* interaction is negligible), Type *II* (dominant *NNN* interaction) and Type *III* (strength of *NNN* interaction significant but less than *NN* interaction). Type *II* antiferromagnetic structure leads to disorder and yields a ferromagnetic *NN* interaction along with an antiferromagnetic *NNN* interaction.[28] The presence of disorder leading to spin glass behavior in Sr_2FeCoO_6 shows that the *NNN* interaction is not negligible in double perovskite systems. SG behavior due to incompatible superexchange interactions and magnetic frustration was observed in double perovskites like Sr_2FeTiO_6 (Ref. 22) and Sr_2FeTaO_6.[6] Since Fe^{3+} and Co^{4+} are isoelectronic, they interact ferromagnetically through the *NN* Fe-O-Co superexchange interaction. However, presence of like-pairs of Fe and Co leads to Fe-O-Co-O-Fe *NNN* antiferromagnetic superexchange interaction also.[21] The competition between the *NN* and *NNN* interactions is the origin of the magnetic frustration in Sr_2FeCoO_6, which results in a spin glass state. One of the structural aspects affecting the strength of the nearest neighbor interaction is B-O-B′ angle. The *NN* interaction is stronger if the Fe-O-Co bond angle is near to or equal to 180° in which case, a ferromagnetic interaction manifests. A deviation from the linear Fe-O-Co chain in the case of Sr_2FeCoO_6 was clear from the bond angle value equal to 177.92°. This indicates weak *NN* interaction and also explains the low T_c and magnetic moment values for Sr_2FeCoO_6.

IV. CONCLUSIONS

Sr_2FeCoO_6 synthesized using sol-gel method crystallizes in tetragonal *I*4/*m* structure with disordered cation occupancy. Using neutron diffraction studies, we have confirmed the crystal structure and the subsequent bond valence sums confirm mixed valence for Fe and Co. The different valences of Fe and Co and their mixed occupation in the lattice leads to competition between *NN* and *NNN* exchange interactions, which is also supported by the estimated bond angle values. dc magnetization measurements show irreversibility at ~ 75 K where the spin glass phase sets in. The weak component of ferromagnetism observed in magnetization can be due to the competing antiferromagnetic and ferromagnetic interactions and is clear from the low values of remnance. The spin glass state in Sr_2FeCoO_6 is further supported by the frequency dependence of real component of ac susceptibility. Dynamical scaling analysis confirms the spin glass phase with $T_{ct} = 75.14(8)$ K. We propose that spin glass behavior in Sr_2FeCoO_6 is due to the magnetic frustration resulting from the competing *NN* and *NNN* interactions, which originate from mixed occupation of cations sites. Our work emphasizes that the cationic disorder leads to a spin glass state. The structural and magnetic studies also lead to the deduction of the spin states of Fe and Co in Sr_2FeCoO_6.

ACKNOWLEDGMENTS

The authors acknowledge the Department of Science and Technology (DST), India for financial support for providing the facilities used in this study (Grant Nos. SR/FST/PSII-002/2007 and SR/NM/NAT-02/2005). P.R wishes to thank M. Angst and K. Balamurugan for fruitful discussions.

[1]D. Serrate, J. M. De Teresa, and M. R. Ibarra, J. Phys.: Condens. Matter **19**, 023201 (2007).
[2]D. D. Sarma, E. V. Sampathkumaran, S. Ray, R. Nagarajan, S. Majumdar, A. Kumar, G. Nalini, and T. N. Guru Row, Solid State Commun. **114**, 465 (2000).
[3]M. T. Anderson, K. B. Greenwood, G. A. Taylor, and K. R. Poeppelmeier, Prog. Solid State Chem. **22**, 197 (1993).
[4]J. Gopalakrishnan, A. Chattopadhyay, S. B. Ogale, T. Venkatesan, R. L. Greene, A. J. Mills, K. Ramesha, B. Hannoyer, and G. Marest, Phys. Rev. B **62**, 9538 (2000).
[5]S. Streule, A. Podlesnyak, J. Mesot, M. Medarde, K. Conder, E. Pomjakushina, E. Mitberg, and V. Kozhevnikov, J. Phys.: Condens. Matter **17**, 3317 (2005).
[6]E. J. Cussen, J. F. Vente, P. D. Battle, and T. C. Gibb, J. Mater. Chem. **7**, 459 (1997).
[7]K. -I. Kobayashi, T. Okuda, Y. Tomioka, T. Kimura, and Y. Tokura, J. Magn. Magn. Mater. **218**, 17 (2000).
[8]P. D. Battle, T. C. Gibb, C. W. Jones, and F. Studer, J. Solid State Chem. **78**, 281 (1989).
[9]A. Poddar, R. N. Bhowmik, I. P. Muthuselvam, and N. Das, J. Appl. Phys. **106**, 073908 (2009).
[10]H. Kawanaka, I. Hase, S. Toyama, and Y. Nishihara, Physica B **281**, 518 (2000).
[11]J. Navarro, L. Balcells, F. Sandiumenge, M. Bibes, A. Roig, B. Martínez, and J. Fontcuberta, J. Phys.: Condens. Matter **13**, 8481 (2001).
[12]L. Balcells, J. Navarro, M. Bibes, A. Roig, B. Martínez, and J. Fontcuberta, Appl. Phys. Lett. **78**, 781 (2001).
[13]M. García-Herníandez, J. Martínez, M. J. Martínez-Lope, M. T. Casais, and J. A. Alonso, Phys. Rev. Lett. **86**, 2443 (2001).
[14]H. Sakuma, T. Taniyama, Y. Kitamoto, and Y. Yamazaki, J. Appl. Phys. **93**, 2816 (2003).
[15]A. Maignan, C. Martin, N. Nguyen, and B. Raveau, Solid State Sci. **3**, 57 (2001).
[16]P. Bezdicka, L. Fournés, A. Wattiaux, J. C. Grenier, and M. Pouchard, Solid State Commun. **91**, 501 (1994).
[17]T. Takeda and H. Watanabe, J. Phys. Soc. Jpn. **33**, 973 (1972).
[18]S. Kawasaki, M. Takano, and Y. Takeda, J. Solid State Chem. **121**, 174 (1996).
[19]V. V. Bannikov, I. R. Shein, V. L. Kozhevnikov, and A. L. Ivanovskii, J. Struc. Chem. **49**, 781 (2008).
[20]A. Poddar and C. Mazumdar, J. Appl. Phys. **106**, 093908 (2009).

[21]E. N. Caspi, J. D. Jorgensen, M. V. Lobanov, and M. Greenblatt, Phys. Rev. B **67**, 134431 (2003).
[22]T. C. Gibb, P. D. Battle, S. K. Bollen, and R. J. Whitehead, J. Mater. Chem. **2**, 111 (1992).
[23]J. A. Mydosh, *Spin Glasses: An Experimental Introduction* (Taylor and Francis, London, 1993).
[24]I. G. Deac, S. V. Diaz, B. G. Kim, S. W. Cheong, and P. Schiffer, Phys. Rev. B **65**, 174426 (2002).
[25]H. M. Rietveld, J. Appl. Cryst. **2**, 65 (1969).
[26]J. Rodriguez-Carvajal, Physica B **192**, 55 (1993).
[27]D. C. Wallace, *Thermodynamics of Crystals* (Dover, New York, 1998).
[28]L. Ortega-San Martin, J. P. Chapman, L. Lezama, J. J. S. Garitaonandia, J. S. Marcos, J. Rodríguez-Fernández, M. I. Arriortua, and T. Rojo, J. Mater. Chem. **16**, 66 (2006).
[29]*Data From Neutron News* **3**, 29 (1992), URL http://www.ncnr.nist.gov/resources/n-lengths.
[30]R. Pradheesh, H. S. Nair, A. T. Satya, A. Bharathi, R. Nirmala, K. Sethupathi, and V. Sankaranarayanan, "Large magnetoresistance and Jahn-Teller effect in Sr_2FeCoO_6" (to be published).
[31]A. S. Wills and I. D. Brown, VaList- Bond Valence Calculation and Listing; program is available from www.ccp14.ac.uk.
[32]J. Blasco, C. Ritter, L. Morellon, P. A. Algarabel, J. M. De Teresa, D. Serrate, J. García, and M. R. Ibarra, Solid State Sci. **4**, 651 (2002).
[33]A. M. Glazer, Acta Crystallogr. B **28**, 3384 (1972).
[34]R. D. Shannon, Acta Crystallogr. Sect. A **32**, 751 (1976).
[35]H. Taguchi, M. Shimada, and M. Koizumi, J. Solid State Chem. **29**, 221 (1979).
[36]P. G. Radaelli and S. W. Cheong, Phys. Rev. B **66**, 094408 (2002).
[37]J. B Goodenough, Phys. Rev. **100**, 564 (1955).
[38]J. Kanamori, J. Phys. Chem. Solids **10**, 87 (1959).
[39]G. Cao, Y. Xin, C. S. Alexander, and J. E. Crow, Phys. Rev. B **63**, 184432 (2001).
[40]K. V. Rao, M. Fähnle, E. Figueroa, O. Beckman, and L. Hedman, Phys. Rev. B, **27** 3104 (1983).
[41]A. Muñoz, J. A. Alonso, M. J. Martìnez-Lope, C. de La Calle, and M. T. Fernàndez-Dàaz, J. Solid State Chem. **179**, 3365 (2006).
[42]A. A. Wagh, P. S. Anil Kumar, H. L. Bhat, and S. Elizabeth, J. Phys.: Condens. Matter **22**, 026005 (2010).
[43]J. W. Lynn, R. W. Erwin, J. A. Borchers, Q. Huang, A. Santoro, J. L. Peng, and Z. Y. Li, Phys. Rev. Lett. **76**, 4046 (1996).
[44]R. I. Dass and J. B. Goodenough, Phys. Rev. B **67**, 14401 (2003).
[45]H. Kato, T. Okuda, Y. Okimoto, Y. Tomioka, K. Oikawa, T. Kamiyama, and Y. Tokura, Phys. Rev. B **69**, 184412 (2004).
[46]J. L. Tholence, Solid State Commun. **88**, 917 (1993).
[47]K. Gunnarsson, P. Svedlindh, P. Nordblad, L. Lundgren, H. Aruga, and A. Ito, Phys. Rev. Lett. **61**, 754 (1988).
[48]X. Luo, W. Xing, Z. Li, G. Wu, and X. Chen, Phys. Rev. B **75**, 054413 (2007).
[49]M. Viswanathan and P. S. Anil Kumar, Phys. Rev. B **80**, 012410 (2009).
[50]M. Abbate, G. Zampieri, J. Okamoto, A. Fujimori, S. Kawasaki, and M. Takano, Phys. Rev. B **65**, 165120 (2002).
[51]P. D. Battle, and W. J. Macklin, J. Solid State Chem. **52**, 138 (1984).
[52]S. J. Makowski, J. A. Rodgers, P. F. Henry, J. P. Attfield, and J.-W. G. Bos, Chem. Mater. **21**, 264 (2008).
[53]J.-W. G. Bos, and J. P. Attfield, Phys. Rev. B **70**, 174434 (2004).